

Integrated approach for snowmelt run-off estimation using temperature index model, remote sensing and GIS

S. P. Aggarwal*, Praveen K. Thakur, Bhaskar R. Nikam and Vaibhav Garg

Water Resources Department, Indian Institute of Remote Sensing Dehradun, 4-Kalidas Road, Dehradun 248 001, India

The snow and glacier melt run-off is one of the most important sources of freshwater for the perennial Himalayan rivers. The water from these rivers sustains billions of people in South Asia, especially during lean season. The study has been done to integrate temporal snow cover area (SCA) and digital elevation model (DEM) derived from satellite remote sensing data with Geographic Information System (GIS) and finally into temperature index-based snowmelt run-off estimation model. The study area for snowmelt run-off estimation is part of head reach sub-basins of Ganga river, i.e. Alakhnanda and Bhagirathi river basins up to Joshimath and Uttarkashi respectively. The temporal SCA (2002–07 for Bhagirathi river and 2000, 2008 for Alakhnanda river) was derived from remote sensing data and DEM was used to find elevation zones and aspect maps. Snowmelt run-off model (SRM) is a temperature index-based snowmelt run-off simulation model, which has been used in this study for simulating snowmelt run-off. The daily hydro meteorological data from India Meteorological Department and Central Water Commission were used for estimating snowmelt. Overall accuracy of SRM for Alakhnanda river in terms of coefficient of correlation (R^2) is 0.84–0.90 for years 2000 and 2008, and 0.74–0.84 in Bhagirathi river for 2002–2007.

Keywords: Remote sensing, snowmelt run-off, snow cover area, temperature index model.

THE Himalayan region is now popularly known as the ‘third pole’, as the seasonal snow cover and permanent ice fields of its glaciers are the largest outside the polar region. The region contains the world’s highest mountains, including all 14 peaks above 8000 m. This area is the source of 10 major rivers which are fed by the melting of snow and glaciers of this region and more than 3 billion people are benefitted by the food and energy produced in these river basins (<http://www.icimod.org/?q=3487>). During the last 100 years, this area has undergone many changes in land use and land cover, including climate change. The changes in climatic conditions of this region have a direct effect on snowmelt run-off

(SMR) and glacier mass balance¹. In India, the perennial Himalayan rivers are fed by snowmelt and glacier melt run-off². The regular mapping and monitoring of snow cover and glaciers remain a challenge in these hilly areas due to inaccessibility and few ground observation sites. Therefore, considering the importance of seasonal snow cover, glaciers and their associated melt run-off of this region, the present study has been made to achieve the objective of integrating temperature index model³ for SMR estimation with remote sensing and Geographic Information System (GIS).

Remote sensing for snow cover mapping and SMR modelling

Satellite imagery has been successfully used for snow cover area (SCA) mapping and is employed in many studies to improve the performance of numerical models that predict SMR^{4–7}. Snow cover is one of the most easily recognized features in the visible spectrum of the satellite image as it can be distinguished from other objects on the Earth’s surface due to its relative high albedo and reflectance (Figure 1). As a result, determination of the extent of the snow cover was one of the early accomplishments of satellite data interpretation. In 1960 Singer and Popham⁸ had observed snow in the first image obtained from the TIROS-1 satellite. With the help of remote sensing

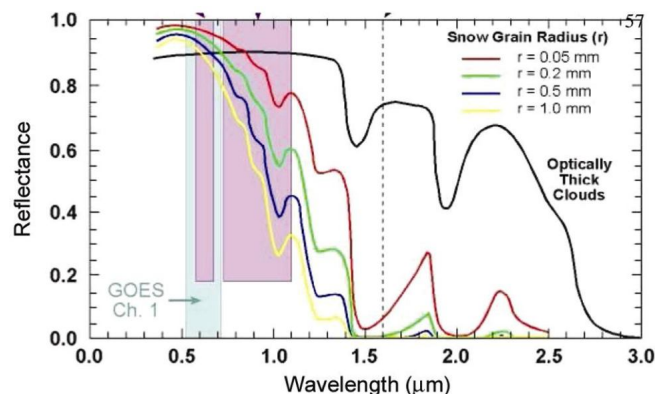


Figure 1. Reflectance spectra for snow and clouds (http://nsidc.org/data/docs/daac/nsidc0066_avhrr_5km.gd.html).

*For correspondence. (e-mail: spa@iirs.gov.in)

data, various types of snow classes⁹ (fresh dry snow, old wet snow, etc.) can easily be mapped and monitored. Optical remote sensing, which works in the visible to infrared region of the electromagnetic (EM) spectrum, has been used effectively to map the SCA¹⁰⁻¹⁹, and these SCA maps have been used in SMR studies²⁰⁻²⁶.

The most common method for SCA mapping using optical multi-spectral images is to use the band ratio method. This method uses a spectral band in the visible part of the spectrum, plus one centred near 1.65 μm in the middle infrared (MIR)^{12,27-29}. These bands are selected as the spectral reflectance of snow cover and cloud are similar at wavelengths below about 1 μm , and they diverge in the near infrared (NIR) and achieve a maximum difference (as cloud is more reflective than snow) at wavelengths between about 1.55 and 1.75 μm . For the discrimination of snow, this band ratio index is called the normalized difference snow index (NDSI), which was originally defined in terms of the spectral bands of Landsat Thematic Mapper (TM) and Enhanced Thematic Mapper (ETM+) as

$$\text{NDSI} = (R_2 - R_5)/(R_2 + R_5), \quad (1)$$

where R_2 and R_5 are the reflectances in bands 2 and 5 (centre wavelengths 0.57 and 1.65 μm) respectively^{12,13}. Snow is normally assumed to be present if the NDSI exceeds a value of 0.4 (refs 14, 16), although recent studies have suggested that the optimum value of the threshold varies seasonally³⁰. The regular mapping and monitoring of snow cover in the Indian Himalayas has been done using optical remote sensing data of Indian Remote Sensing Satellite (IRS), Resourcesat-1 and Moderate Resolution Imaging Spectroradiometer (MODIS)^{17,18,31}.

Macchiavello *et al.*³² have classified the snow-covered areas from multi-spectral images (MODIS and LANDSAT). This study was based on integration of decision tree classifier and a Bayesian unsupervised thresholding algorithm in order to automatically choose an optimal threshold to be applied to NDSI. Roshani *et al.*³³ classified glaciers using IRS-LISS (III) and LANDSAT data. Distinguishing of snowy and no-snowy zones was done using NDSI index with a value of 0.3 as threshold. To obtain new snow, scatter plot of bands 2, 4 of LANDSAT was used as fresh snow has high reflectance in these bands, while for old snow extraction, bands 4, 5 were used as old snow has low reflectance in these bands. In the context of the Indian Himalayas, remote sensing-based snow cover has been used in estimating the SMR for few river basins and other snow hydrology-related studies²²⁻²⁶.

Snowmelt run-off model

Hydrological models used for simulation or forecasting of stream flow are generally categorized as simple regres-

sion models, black-box models, conceptual models and physically based models³⁴. In general, snowmelt models can be divided into two types, namely energy balance models and temperature index models^{35,36}. The other method of SMR estimation, which is based on isotope analysis, has been used in recent studies in parts of Western Himalayas^{37,38}.

The energy balance or the heat budget of a snowpack governs the production of melt water. This method involves accounting for a given period of time, the net incoming and outgoing energy in short wave and long wave, and the changes in the energy storage for a snowpack. The net energy is then expressed as the heat equivalent of snowmelt. The presence of cloud cover and vegetation cover significantly affects the energy balance of a snow surface. The energy balance models require a large amount of well-distributed hydrometeorological data to set up the model and simulate the SMR. As well-distributed hydrometeorological data in the Indian Himalayas are scanty, only few studies have been done in India for estimating SMR using energy balance approach^{39,40}.

In the temperature index models, mainly daily air temperature data are used along with degree day factor and snow cover information to simulate the daily SMR. These have been used extensively and with fair degree of accuracy in data-scarce Indian Himalayan catchments^{22-26,41}. As the study area of Ganga Basin has less hydrometeorological data, the present study has used temperature index modelling approach for estimating SMR. Details of the model used and its structure are given in the next section.

Temperature index model for SMR: The most popular temperature index method used is SRM by Martinec³ in 1975. This was developed in small European basins originally and has been used in many parts of the world in mountain basins of almost any size and any elevation range³⁵. The structure of the model is as follows:

$$Q_{n+1} = [C_{S_n} a_n (T_n + \Delta T_n) S_n + C_{R_n} P_n] * A \\ * (10000/86400) * (1 - K_{n+1}) + Q_n K_{n+1},$$

where Q is the average daily discharge [$\text{m}^3 \text{s}^{-1}$], C the run-off coefficient expressing the losses as a ratio (run-off/precipitation), with C_S referring to snowmelt and C_R to rainfall, a the degree-day factor [$\text{cm } ^\circ\text{C}^{-1} \text{d}^{-1}$] indicating the snowmelt depth resulting from 1 degree-day, T the number of degree-days [$^\circ\text{C d}$], ΔT the adjustment by temperature lapse rate when extrapolating the temperature from the station to the average hypsometric elevation of the basin or zone [$^\circ\text{C d}$], S the ratio of the snow covered area to the total area and P the precipitation contributing to run-off (cm). A pre-selected threshold temperature, T_{CRIT} , determines whether this contribution is from rainfall or snowfall. If precipitation is determined

by T_{CRIT} to be new snow, it is kept on storage over the hitherto snow-free area until melting conditions occur. In the above equation, A is the area of the basin or zone (km^2), K_{n+1} the recession coefficient indicating the decline of discharge in a period without snowmelt or rainfall: $K = Q_{n+1}/Q_n$ ($n, n+1$ are the sequence of days during a true recession flow period), n the 130 sequence of days during the discharge computation period and 10000/86400 is the conversion from $\text{cm km}^2 \text{d}^{-1}$ to $\text{m}^3 \text{s}^{-1}$. The well-known watershed models, viz. hydrological modelling system (HMS), precipitation run-off modelling system (PRMS), and soil and water assessment tool (SWAT) have similar or modified temperature index options⁴². This temperature index model-based SMR method has been used in Himalayan river basins such as Beas Basin up to Pandoh²⁵, up to Manali^{26,41,42}, and other rivers basins of the Himalaya^{38,43-46}.

Study area

The study area is the upper Ganga catchment with main emphasis on Alakhnanda and Bhagirathi basins. Alakhnanda up to Joshimath and Bhagirathi up to Uttarkashi have been considered in this study (Figure 2 a-c). The Alakhnanda Basin extends between $30^{\circ}0'-31^{\circ}0'N$ and $78^{\circ}45'-80^{\circ}0'E$ covering an area of about 4533.32 km^2 , with elevation ranging from 1450 to 7771 m amsl and represents the eastern part of Garhwal Himalaya. About 433 km^2 of the total area of the basin is under glacier landscape and 288 km^2 is under fluvial landscape. The Bhagirathi river basin is situated in Uttarakhand, within geographical coordinates $30^{\circ}38'-31^{\circ}24' N$ lat. and $78^{\circ}29'-79^{\circ}22' E$ long. with area of 4495.52 km^2 up to Uttarkashi. The altitude variation is from 1121 to 7000 m amsl. The Alakhnanda and Bhagirathi river basins are characterized predominantly by hilly terrain, deep gorges and river valleys. The region broadly falls under four major divisions: (i) the Great Himalayan Ranges (snow-covered regions), (ii) Alpine and pasture land (covered by snow during four months of the winter season), (iii) Middle Himalaya (characterized by highest population) and (iv) river valleys (characterized by service centres and institutions). Among the major rivers of India, the Alakhnanda and its tributaries (Dhaulti Ganga, Vishnu Ganga, Nandakini, Pindar, Mandakini and other numerous perennial streams) originate and flow in this river basin⁴⁷. The highest mountain peaks of the Himalayan ranges such as Nandadevi, Kamet, Trisul and Chaukhamba are located in the Alakhnanda river basin⁴⁸.

The headwaters of the Bhagirathi are formed at Gaumukh (elevation 3892 m), at the foot of the Gangotri and Khatling in the Garhwal Himalaya (http://en.wikipedia.org/wiki/Bhagirathi_River). It is then joined by its tributaries; these are, in order from the source: Kedar Ganga at Gangotri (elevation 3049 m), Jadh Ganga at

Bhaironghati (elevation 2650 m), Kakora Gadand Jalandhari Gad near Harsil (elevation 2745 m), Siyan Gad near Jhala (elevation 2575 m), Asi Ganga near Uttarkashi (elevation 1158 m) and Bhilangna River near old Tehri (elevation 755 m). The Bhilangna itself rises at the foot of the Khatling glacier (elevation 3717 m), approximately 50 km south of Gaumukh (http://en.wikipedia.org/wiki/Bhagirathi_River). The river flows from its source for 205 km before meeting the Alakhnanda river at an elevation of 475 m in the town of Devprayag. After Devprayag, the river is known as the Ganga or Ganges river (http://en.wikipedia.org/wiki/Bhagirathi_River).

Data used and methodology

The main remote sensing and digital elevation data used in this study are given in Table 1. Details of each data type are given in subsequent sections. Details on the hydrometeorological data are given later in the text. The overall methodology flowchart is given in Figure 3.

Remote sensing data

The SCA in the Bhagirathi river basin was determined during the period 2002–07 using MODIS, and also using Landsat data for the year 2000 and Advanced Wide Field Sensor (AWiFS) data for the year 2008 in Alakhnanda river basin. MODIS is a key instrument aboard the Terra (EOS AM) and Aqua (EOS PM) satellites. The orbit of these satellites around the Earth is timed so that Terra passes from north to south across the equator in the morning, while Aqua passes from south to north over the equator in the afternoon. The MODIS instrument provides high radiometric sensitivity (12 bit) in 36 spectral bands ranging in wavelength from 0.4 to $14.4 \mu\text{m}$ (<http://modis.gsfc.nasa.gov/about/>). The eight-day climate-modelling grid (CMG) snow cover data product is generated by merging all the MOD10C2 products for an eight-day period and binning that 500 m data to $1/20^{\circ}$, or about 5.6 km resolution to create a global CMG map of snow cover (<http://modis-snow-ice.gsfc.nasa.gov/?c=MOD10C2>). The size of the arrays is 3600 rows by 7200 columns. Snow cover, cloud cover and quality assurance information are included in the product.

The cloud-free time series of IRS-P6 or AWiFS of Resourcesat-1 (<http://www.isro.org/satellites/irsp6resource-sat-1.aspx>) and Landsat Enhanced Thematic Mapper (ETM+) (<http://landsat.usgs.gov/about/landsat7.php>) data have been used to estimate SCA for Alakhnanda basin. Selection of optimal date of AWiFS and Landsat imagery was done taking into consideration the months with maximum (February–March) and minimum (September–December) snow cover and availability of cloud-free imagery. All images were registered to the UTM projection in WGS 84 North datum with zone 44. All full SCA data

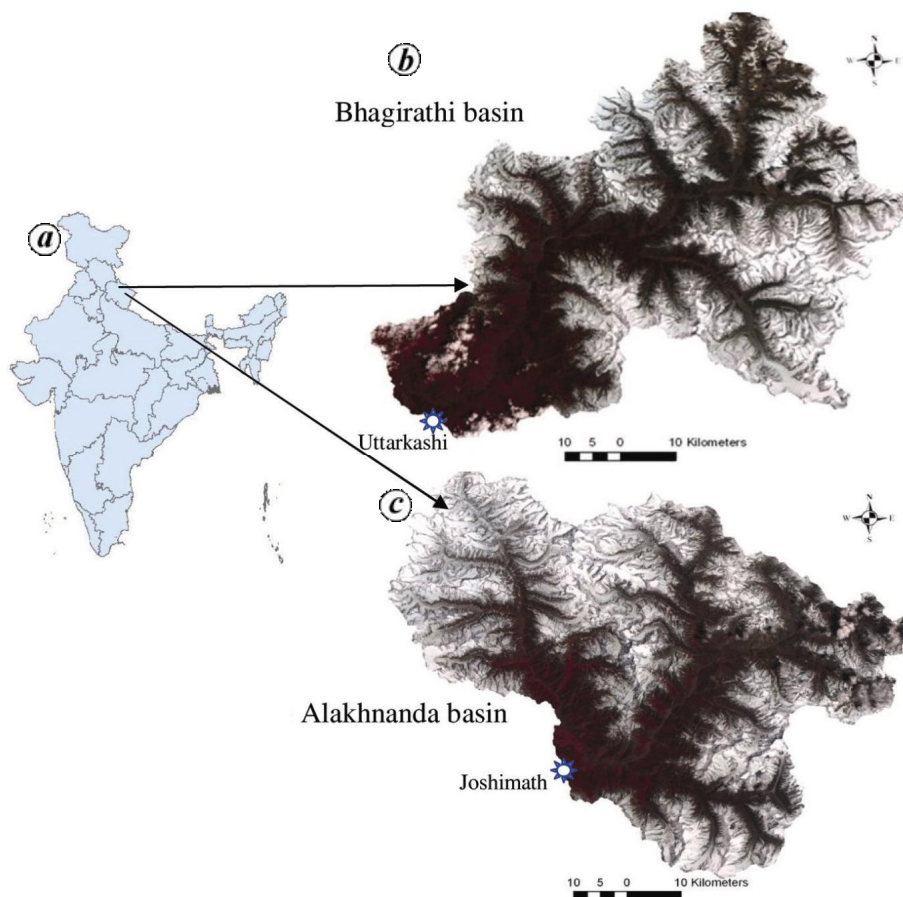


Figure 2. *a*, Location map of Uttarakhand, India with AWiFS image-based colour composite. *b*, Bhagirathi river basin up to Uttarkashi. *c*, Alakhnanda river basin up to Joshimath.

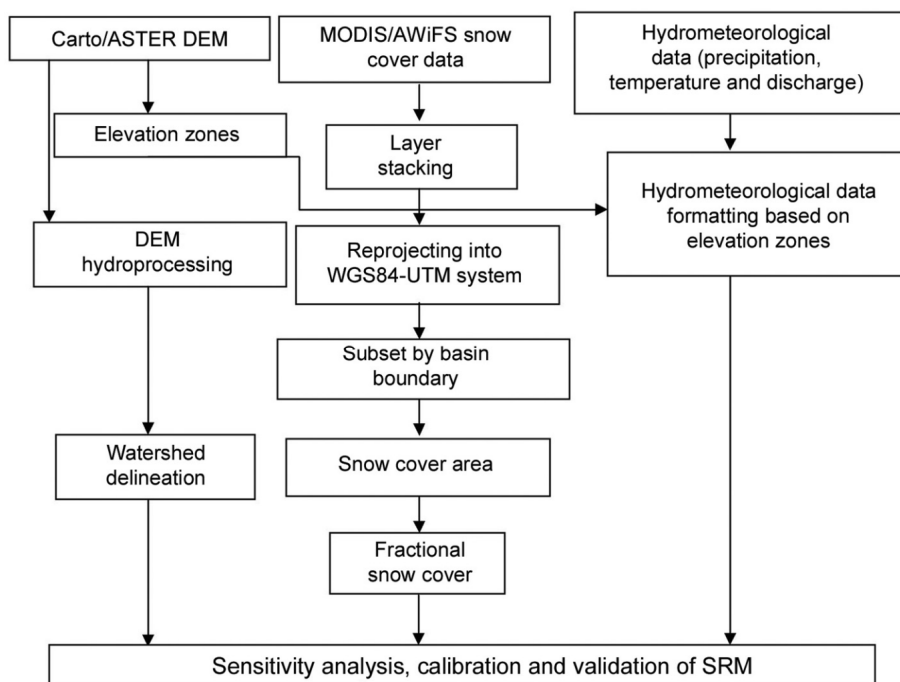


Figure 3. Flowchart of the overall methodology.

Table 1. Summary of data used in the study

Satellite	Sensor	Data type	Time-period	Spatial resolution (m)
IRS-P6	AWiFS	Multispectral image	2007–2008	56
TERRA	MODIS	Multispectral image	2002–2007	500
LANDSAT	TM/ETM	Multispectral image	1999–2001	30
ASTER	ASTER	DEM	2008	30

were extracted by basin boundary shape file. Also, radiometric calibration of AWiFS and Landsat data was done to get proper and high-quality data. All radiometric calibration steps are described later in the text.

Advanced Space-borne Thermal Emission and Reflection Radiometer (ASTER) sensor is one of the five remote sensory devices on-board the Terra satellite launched into the Earth's orbit by NASA in 1999. ASTER GDEM (Global Digital Elevation Model)⁴⁹ is the global DEM created using ASTER (<http://gdem.ersdac.jspacesystems.or.jp/>).

Hydrometeorological data

Hydrometeorological data requirement for the study area include: maximum, minimum and average temperature, precipitation and run-off (discharge). Discharge and meteorological data for time-period 2000–09 have been collected. Meteorological data were available from Automatic Weather Station (AWS) of Indian Space Research Organisation (ISRO) located near Harsil, Uttarkashi and near Joshimath. All other data have been provided by India Meteorological Department (IMD), New Delhi; National Institute of Hydrology (NIH), Roorkee, and Central Water Commission (CWC), Dehradun.

Methodology

The overall methodology flowchart is given in Figure 3. As part of remote sensing data preprocessing, digital number to top-of-atmosphere (TOA) reflectance was also calculated. Calculation of at-sensor spectral radiance is the fundamental step for converting image data into a meaningful common radiometric scale. During radiometric calibration, pixel values are converted to units of absolute spectral radiance using 32-bit floating-point calculations and this radiance is converted to at-sensor spectral reflectance or TOA reflectance. This is required to reduce scene-to-scene variability and is done using standard procedure given in the literature⁵⁰.

For mapping and monitoring of temporal snow cover, the NDSI method was used^{12,13}. NDSI uses the high and low reflectance of snow in visible (green) and short-wave infrared (SWIR) respectively, and it can also delineate the snow in mountain shadows. After NDSI is calculated,

the threshold is found by visual inspection of the image and sampling NDSI values. In our study the NDSI threshold values for AWiFS and LANDSAT were taken in the range 0.4–0.5. MODIS-based SCA is also based on the NDSI method¹⁶.

The ASTER GDEM was used to create the elevation bands or zones (Figure 4 *a* and *b*) for the selected river basin of the study area. For simulation of SMR, the Bhagirathi basin was divided into seven elevation zones ranging from 1200 to 7500 m. Most of the area belongs to the fifth elevation zone (4500–5500 m) and consists of 43.67% of total area (1966.52 km²), whereas minimum area 0.39% (17.58 km²) is in the seventh elevation zone with elevation ranging from 6500 to 7500 m. Similarly, six elevations zones ranging from 1450 to 7771 m were created for Alakhnanda basin using ASTER GDEM (Figure 4 *b*).

In Alakhnanda river basin, a large part of the area belongs to fourth and fifth elevation zones (4000–5000 m and 5000–6000 m) and consists of 36.80% and 39.50% of total area (1667.55 and 1791.11 km²) respectively, whereas the minimum area 0.6% (26.02 km²) is in the first elevation zone with elevation ranging from 1450 to 2000 m. These elevation zone maps are used in zonal statistics tool of GIS for estimation of fractional SCA in each zone, as well as the maximum and minimum temperature and rainfall (IMD's meteorological data up to 2005 was available in grid format).

Results and discussion

Snow cover area mapping

Figure 5 shows fractional (0 to 1) SCA from 2001 to 2009 for the Bhagirathi river basin. After delineating boundary of the study area, snow cover fraction was calculated by interpolating weekly data of MODIS to daily snow cover data.

Figure 5 shows that accumulation is maximum from December to March due to low temperature and snowfall in higher altitude areas. Similarly, SCA is minimum from July to September because of monsoon and high temperature and follows the same trend from 2001 to 2009. During the period from October to December, snow cover is optimum. Sample images of Landsat FCC with snow

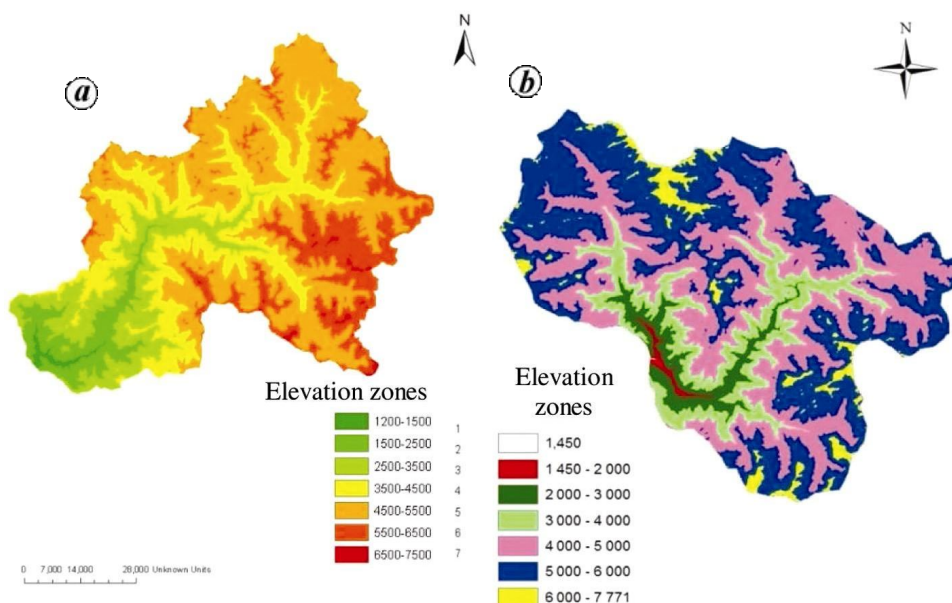


Figure 4. Elevation zone maps. *a*, Bhagirathi basin up to Uttarkashi; *b*, Alakhnanda river basin up to Joshimath.

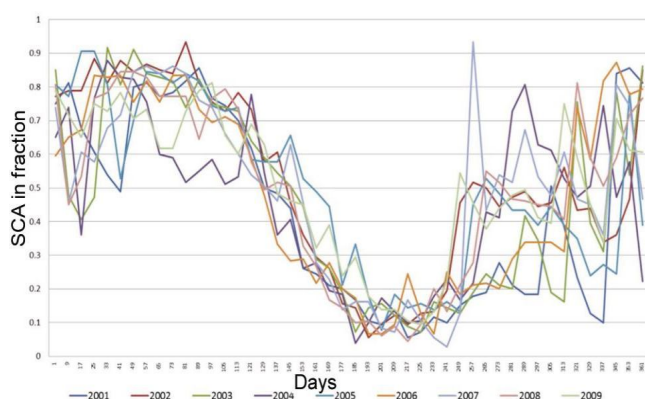


Figure 5. Snow cover area fractions of Bhagirathi river basin.

cover seen in white colour are shown in Figure 6. Similarly, SCA for Alakhnanda river basin has been calculated using AWiFS and Landsat data. The areal extent of seasonal snow cover gradually decreases during the snowmelt season. Figure 7 shows the snow depletion curves in the Alakhnanda basin from Landsat and AWiFS datasets. For SRM, full year 2000 and 2008 data were used for calibration and validation. Elevation zone-wise SCA fractions⁵¹ were calculated for river basins as SRM takes this information for SMR simulation.

The altitude up to 2000 m is not under snow. During 2008, SCA decreased from January to November and in December due to heavy snowfall it increased again. Most of the snow is concentrated at high altitudes, i.e. higher than 5 km. During 2000, SCA increased from the beginning of the year up to April and decreased subsequently up to November. Temperature and precipitation along with depletion curves are used in SRM to simulate SMR.

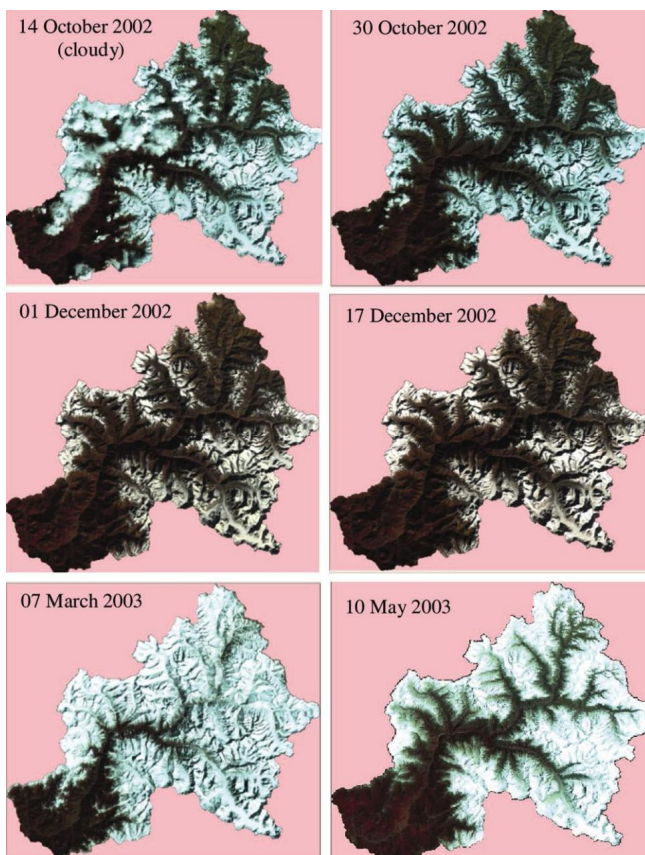
The SCA depletion curves vary significantly from year to year and therefore, the snow cover depletion curve has to be drawn separately for each year. As a result of SCA mapping in Alakhnanda river basin, maximum snow accumulation was on 26 February 2008 (3106 km²) and 10 April 2008 (2733 km²). The minimum snow cover was on 11 November 2008 (272 km²). In 2000, maximum accumulation was in April (3766 km²). As SRM needs daily SCA, the available eight-day or monthly SCA was used with linear interpolation method to get the daily SCA. This method can sometimes over- or underestimate SCA as fresh snowfall before or after satellite pass may not be represented accurately in the method. Overall trend of SCA at seasonal timescale is maintained. For Bhagirathi basin during the study period of 2002–2007, maximum snow accumulation was observed in March 2002, i.e. 4200 km² and minimum in September 2007. During the period from October to December snow cover was about 1600–1800 km².

Result of snowmelt run-off

Bhagirathi basin: In SRM, many parameters need to be parameterized for calibration and validation of SMR. The calculated and calibrated parameters are lapse rate, critical temperature (T_{CRIT}), degree-day factors (a_n), lag time, snow run-off coefficient (C_S), rainfall run-off coefficient (C_R), rainfall contribution area (RCA), X coefficient and Y coefficient as part of recession coefficients. The value of lapse rate varies from 0.65 to 0.75, critical temperature is 2.0°C, degree-day factors from 0.35 to 0.65, lag time is 18.0 h, C_S and C_R vary from 0.10 to 0.80, RCA from 0 to 1, X coefficient from 0.90 to 1.02 and Y coefficient from

Table 2. Sample snowmelt run-off model parameters used for the year 2004

Date	Lapse rate	T_{CRIT}	a_n	Lag time	C_s	C_r	RCA	X_{coeff}	Y_{coeff}
January 2004	0.65	2.00	0.35	18.00	0.10	0.10	0.00	0.90	0.80
February 2004	0.65	2.00	0.35	18.00	0.10	0.10	0.00	0.90	0.80
March 2004	0.65	2.00	0.35	18.00	0.10	0.10	0.00	0.90	0.80
April 2004	0.65	2.00	0.45	18.00	0.10	0.10	1.00	0.90	0.80
May 2004	0.65	2.00	0.55	18.00	0.20	0.20	1.00	0.90	0.80
June 2004	0.65	2.00	0.55	18.00	0.30	0.30	1.00	0.90	0.80
July 2004	0.65	2.00	0.55	18.00	0.55	0.60	1.00	0.90	0.80
August 2004	0.65	2.00	0.65	18.00	0.80	0.80	1.00	0.90	0.80
September 2004	0.65	2.00	0.45	18.00	0.40	0.50	1.00	0.90	0.80
October 2004	0.65	2.00	0.35	18.00	0.20	0.30	0.00	0.90	0.80
November 2004	0.65	2.00	0.35	18.00	0.10	0.10	0.00	0.90	0.80
December 2004	0.65	2.00	0.35	18.00	0.10	0.10	0.00	0.90	0.80

**Figure 6.** Bhagirathi snow as seen in Landsat FCC for the period 2002–2003.

0.80 to 0.88. The sample parameters of SRM are given in Table 2 for the year 2004. The period 2002–2004 was used for calibration and 2005–2007 for validation of SRM.

SRM uses two well-established accuracy criteria, namely the coefficient of determination (R^2) and the volume difference (D_v), which are automatically computed and displayed after each run of SRM. Table 3 shows the results of SRM-based snowmelt.

From the table we can see that R^2 for snowmelt season for 2002–2007 varied from 0.84 to 0.74. Measured run-

off for melt season is about 2751.60–4139.83 (10^6 m^3), average run-off is 87.01–131.27 (m^3/s), computed run-off is 2737.50–4119.16 (10^6 m^3), and computed run-off average 86.57–130.62 (m^3/s). Volume difference varies from 7.54% for 2006 to 0.05% for 2002. Figure 8 shows that SMR started increasing from the spring–summer (April–May) season, mainly due to increase in air temperature, whereas maximum run-off was observed in August, mainly due to monsoonal rains. Snowmelt is low from October to February.

Run-off simulation has been carried out for the Bhagirathi catchment as illustrated. The simulation confirms SMR as the main source of freshwater in the region throughout the year, except during monsoon, when rain on snow and normal rainfall–run-off contribution is much higher than normal SMR due to increase in temperature. The catchment SCA mainly melts in summer and this has caused the computed run-off to increase in these months, similar to that of measured run-off during this period. During winter, especially in December–February, snowmelt is low as a result of low air temperature and degree-days.

In the monsoon season from mid-June to July, rainfall is high and hence computed and measured run-off values are also high. The SRM results are not accurate during monsoon period. As SRM is based on the concept of run-off coefficients of snow and rainfall along with degree-day factor^{52,53}, run-off is directly proportional to rainfall, with run-off coefficients deciding the amount of rainfall being converted to run-off. The main mismatch is between the peaks of measured and computed discharge and time when these peaks occur. To adjust and reduce these errors, recession coefficient is used, which is an important feature of SRM, since $(1 - K)$ is the proportion of the daily melt water production which immediately appears as the run-off^{52,54}. Values of Q_n and Q_{n+1} were plotted against each other in order to determine the K value⁵². For estimating the K values for this study area, the discharge data of Uttarkashi station were used for the period 2002–2007. More calibration is required for X and Y coefficients during monsoon period as the number of peak flows is

Table 3. Results of model simulation for the period 2002–2007 for Bhagirathi basin

Period	2002	2003	2004	2005	2006	2007
Measured run-off volume (10^6 m^3)	4102.93	4139.83	2751.60	3647.82	3647.33	3326.63
Average measured run-off (m^3/s)	130.10	131.27	87.01	115.67	115.66	105.49
Computed run-off volume (10^6 m^3)	4100.97	4119.16	2737.50	3566.63	3372.16	3302.83
Average computed run-off (m^3/s)	130.04	130.62	86.57	113.10	106.93	104.73
Volume difference, D_v (%)	0.05	0.50	0.51	2.23	7.54	0.72
Coefficient of determination, R^2	0.84	0.82	0.76	0.84	0.81	0.74

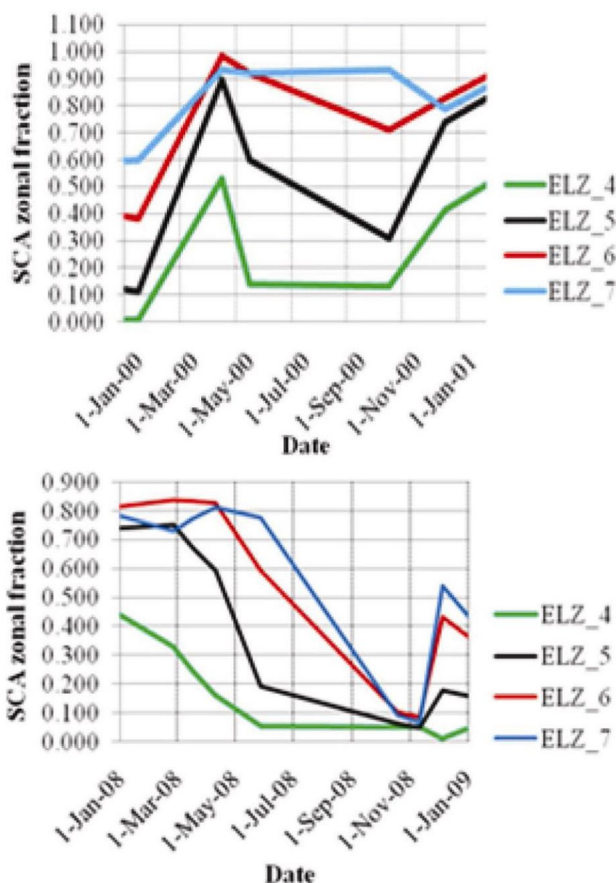


Figure 7. Snow depletion curves for different elevation zones in 2000 and 2008.

more due to many intense rainfall events. Peak discharge values of computed and measured run-off change directly with run-off coefficient and location of flow peaks is mainly governed by X and Y coefficients.

Results of Alakhnanda basin: For calibration and validation of SRM simulation, the years 2000 and 2008 respectively were used. The calibration parameters for this basin are the same as those used in Bhagirathi basin, as the same SRM has been used in both the river basins. For this basin degree day factor was taken from 0.40 to $0.64 \text{ cm}^\circ\text{C}^{-1} \text{ d}^{-1}$. A critical temperature of 0.75°C was assumed and kept constant during the year. If temperature

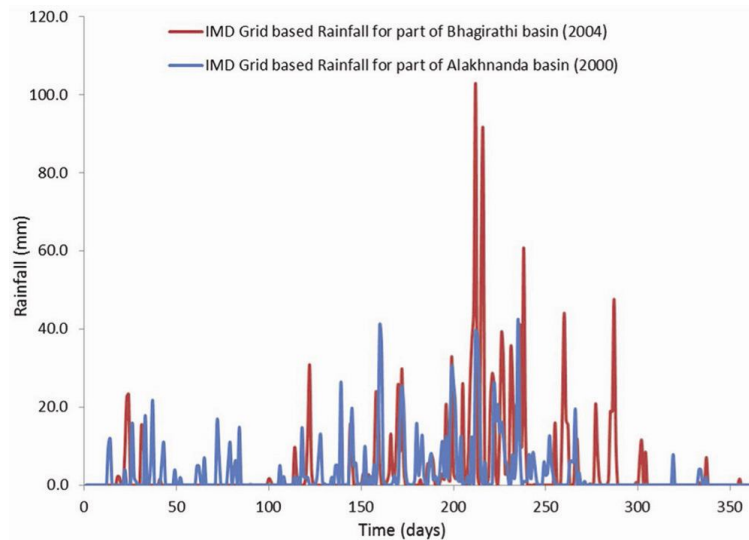
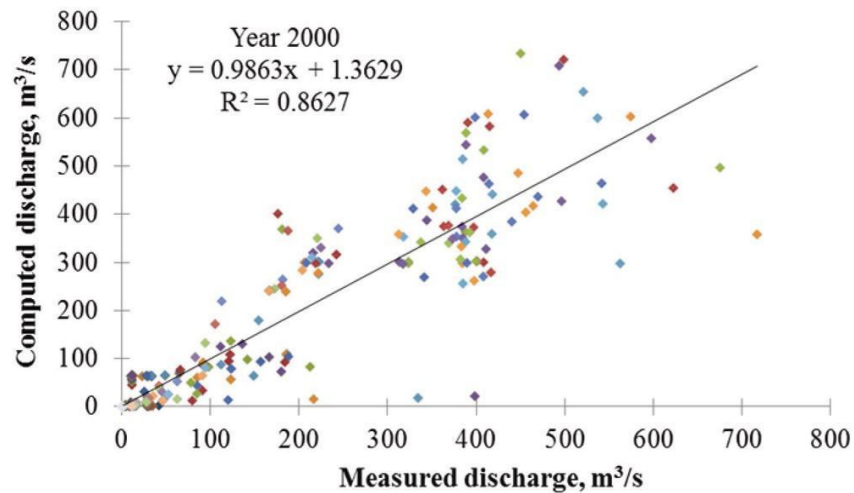
stations at different altitudes are available, the lapse rate can be predetermined from historical data. Otherwise, it must be estimated by comparison from other basins or with similar climatic conditions⁵³. In SRM simulations, a lapse rate of 0.65°C per 100 m is usually employed. In this study, a lapse rate of 0.67°C per 100 m was calculated from IMD data. The run-off coefficients correspond to the ratio of the measured precipitation to the measured run-off. Coefficients are usually different for snowmelt and for rainfall run-off. The run-off coefficients C_S and C_R along with other parameters used by SRM are given in Table 4.

Using the above hydrological and meteorological parameters and daily snow cover estimated from digital image processing of satellite remote sensing data for the given basin, the discharge hydrographs were computed for the Alakhnanda river basin for the entire years 2000 and 2008. The sample observed versus estimated discharges with regression analysis for year 2000 are shown in Figure 9. To analyse the performance of the model, linear regression analysis was performed. R^2 of 0.86 with volume difference of 0.14% was achieved for the year 2000. For validation, the year 2008 was used with the same parameters as those used in the year 2000 simulation. R^2 of 0.84 was achieved for the year 2008, which indicates the existence of a high degree of correlation between measured and computed discharge.

According to the regression between measured and computed run-off values for 2000, R^2 is 0.86 . The catchment in the years 2008 and 2000 has less SCA in summer and heavy rainfall has caused the computed run-off to settle a little lower than measured run-off in this period. In 2008 during winter period computed run-off was slightly higher than measured run-off and this can be due to the intense precipitation events in January and March. The model simulates the run-off peaks with correct delay related to the causing event, but the simulated run-off peaks in 2008 and 2000 are smaller than the measured run-off. This is most probably attributed to the change of run-off coefficient and recession coefficient with time, which could not be accounted for without proper field data. Overall snowmelt simulation for both years is good, with $R^2 = 0.84$ in 2008 and 0.86 in 2000. In spite of these differences, both simulations can be used for SMR calculation, snowmelt forecasting and changed climate scenarios for this area.

Table 4. Model parameters for 2000 and 2008

Model parameter/year	2000	2008
Temperature lapse rate, γ	0.67°C/100 m	0.67°C/100 m
Critical temperature, T_{CRIT}	0.75°C	
Degree-day factor, a	0.40 to 0.64 $\text{cm}^\circ\text{C}^{-1} \text{d}^{-1}$	
Lag time, L	24 h	
Rainfall contributing area (RCA)	March to September = 1; else 0	
Run-off coefficients (C_S for snow, C_R for rainfall)	$C_S = 0.15-0.75$; $C_R = 0.20-0.75$	
Coefficient, X	1.039	1.039
Recession coefficient, Y	0.06	0.01

**Figure 8.** IMD grid-based rainfall for part of Alakhnanda and Bhagirathi basins.**Figure 9.** Measured and simulated discharge of the Alakhnanda river for the year 2000.

Conclusions

Snowmelt run-off modelling for data-scarce Alakhnanda and Bhagirathi river basins is done effectively by integrating remote sensing-based SCA and DEM data, traditional hydrometeorological data in temperature index-

based SRM. The elevation zone approach along with aspect map of the basin improves the quality of SRM simulations as it gives elevation zone-wise input parameters and output SMR. The most sensitive calibration parameters in SRM are degree-day factor, run-off coefficients and recession coefficients.

The dominant SMR is from 15 March to 15 June of a given year, as air temperature gradually increases during this time, which affects SMR⁵⁵. Maximum discharge (snowmelt plus rainfall-run-off) for the period of study is during monsoon season (July and August) and in winter season from October to February snowmelt decreases. The average coefficient of determination for snowmelt season in Bhagirathi basin for the time-period 2002–2007 is 0.80, measurement run-off is about 3602.69 (10⁶ m³), average run-off 114.20 m³, computed run-off 3533.21 (10⁶ m³), average computed run-off 112.00 (m³/s) and volume difference is 1.93. Similarly, for Alakhnanda river basin, overall snowmelt simulation for both years is good, with R² = 0.84 in 2008 and 0.86 in 2000.

Based on this study further improvement can be made for achieving better results using high repeatability of cloud-free optical images along with SCA mapping with SAR^{56–58} images during cloudy conditions, as it has great potential and advantage over optical data during cloud cover and in case of areas under shadow. Incorporating accurate and daily hydrometeorological data in different elevation zones, the SRM results can be compared with other SRMs. As SRM needs only basic meteorological and SCA information and has the capability to simulate changed climate scenarios, the effect of climate change on SMR can be simulated in future studies. Finally, the current approach can be used to operationalize the SMR forecasting in this area using daily SCA data derived from upcoming new sensors (www.isro.org).

1. Adam, J. C., Hamlet, A. F. and Lettenmaier, D. P., Implications of global climate change for snowmelt hydrology in the twenty-first century. *Hydrol. Process*, 2009, **23**(7), 962–972.
2. Singh, P. and Singh, V. P., *Snow and Glacier Hydrology*, Kluwer Academic Publishers, Dordrecht, 2001.
3. Martinec, J., Snowmelt-runoff model for stream flow forecasts. *Nordic Hydrol.*, 1975, **6**(3), 145–154.
4. Ramamoorthi, A. S., Snow cover area (SCA) is the main factor in forecasting snowmelt run-off from major river basins. Large scale effects of seasonal snow cover, Proceedings of the Vancouver Symposium, IAHS Publ. No. 166, 1986, pp. 187–198.
5. Rango, A. and Martinec, J., Application of snowmelt runoff model using Landsat data. *Nordic Hydrol.*, 1979, **10**, 225–238.
6. Rango, A. and Salomonson, V. V., Employment of satellite snow cover observations for improving seasonal run-off estimates. In Proceedings of Workshop on Operational Applications of Satellite snow Cover Observations, Washington DC, 1975, NASA-SP-391, pp. 157–174.
7. Rango, A., Salomonson, V. V. and Foster, J. L., Seasonal stream-flow estimation in the Himalayan region employing meteorological satellite snow cover observations. *Water, Resour. Res.*, 1977, **13**, 109–112.
8. Singer, F. S. and Popham, R. W., Non-meteorological observations from satellites. *Astronaut. Aerosp. Eng.*, 1963, **1**(3), 89–92.
9. Gupta, R. P., Haritashya, U. K. and Singh, P., Mapping dry/wet snow cover in the Indian Himalayas using IRS multi spectral imagery. *Remote Sensing Environ.*, 2005, **97**, 458–469.
10. Andersen, T., Operational snow mapping by satellites. In Proceedings to the Exeter symposium, IAHS Publ. No. 138, July 1982, pp. 149–154.
11. Dhanju, M. S., Studies of Himalayan snow cover area from satellites. In Proceedings of Symposium on Hydrological Applications of Remote Sensing and Remote Data Transmission (ed. Goodison, B. E.), Hamburg, IAHS Publ. No. 145, August 1983, pp. 401–409.
12. Dozier, J., Snow reflectance from Landsat-4 thematic Mapper. *IEEE Trans. Geosci. Remote Sensing*, 1984, **22**, 323–328.
13. Dozier, J. and Marks, D., Snow mapping and classification from Landsat Thematic Mapper (TM) data. *Ann. Glaciol.*, 1987, **9**, 97–103.
14. Dozier, J., Spectral signature of alpine snow covers from the Landsat thematic mapper. *Remote Sensing Environ.*, 1989, **28**, 9–22.
15. Dozier, J. and Frew, J., Computational provenance in hydrologic science: a snow mapping example. *Philos. Trans. R. Soc. London, Ser. A*, 2009, **367**, 1021–1033.
16. Hall, D. K., Riggs, G. A., Salomonson, V. V., DiGirolamo, N. E. and Bayr, K. J., MODIS snow cover products, *Remote Sensing Environ.*, 2002, **83**, 181–194.
17. Kulkarni, A. V., Singh, S. K., Mathur, P. and Mishra, V. D., Algorithm to monitor snow cover using AWiFS data of Resourcesat-1 for the Himalayan region. *Int. J. Remote Sensing*, 2006, **27**, 2449–2457.
18. Kulkarni, A., Rathore, B. P., Singh, S. K. and Ajai, A., Distribution of seasonal snow cover in central and western Himalaya. *Ann. Glaciol.*, 2010, **51**(54), 121–128.
19. Tait, A. B., Hall, D. K., Foster, J. L. and Armstrong, R. L., Utilizing multiple datasets for snow-cover mapping. *Remote Sensing Environ.*, 2000, **72**, 111–126.
20. Aggarwal, K. C., Kumar, V. and Dass, T., Snowmelt run-off for a catchment of Beas Basin. In Proceedings of the First National Symposium on Seasonal Snow Cover, SASE, Manali, 28–30 April 1983, vol. II, pp. 43–63.
21. Engeset, R. V., Udnæs, H. C., Guneriusson, T., Koren, H., Malnes, E., Solberg, R. and Alfnes, E., Satellite-observed SCA in a run-off model. *Nordic Hydrol.*, 2003, **34**, 281–294.
22. Jain, S. K., Goswami, A. and Saraf, A. K., Snowmelt run-off modelling in a Himalayan basin with the aid of satellite data. *Int. J. Remote Sensing*, 2010, **31**(24), 6603–6618.
23. Kumar, V. S., Paul, P. R., Rao, R., Haefner, H. and Siedel, K., Snowmelt runoff forecasting studies in Himalayan basins. In Proceedings of Kathmandu Symposium, November 1992, Snow and Glacier hydrology. IAHS publication No. 218, 1993, pp. 85–94.
24. Singh, P., Jain, S. K. and Kumar, N., Estimation of snow and glacier contribution to the Chenab River, Western Himalaya. *Mt. Res. Dev.*, 1997, **17**(1), 49–56.
25. Prasad, V. H. and Roy, P., Estimation of snowmelt runoff in Beas Basin, India. *Geocarto Int.*, 2005, **20**(2), 41–47.
26. Thakur, P. K., Aggarwal, S. P. and Radchenko, Y., Snowmelt run-off and climate change studies in Manali sub-basin of Beas river, India. In Proceedings of National Symposium on Climate Change and Water Resources in India, NIH Roorkee, 18–19 November 2009.
27. Massom, R., *Satellite Remote Sensing of Polar Regions: Applications, Limitations and Data Availability*, Belhaven Press, London, and Lewis Publishers (CRC Press), Boca Raton, USA, 1991.
28. König, M., Winther, J. G. and Isaksson, E., Measuring snow and glacier ice properties from satellite. *Rev. Geophys.*, 2001, **39**(1), 1–27.
29. Engman, E. T. and Gurney, R. J., *Remote Sensing in Hydrology*, Chapman and Hall, 1992.
30. Vogel, S. W., Usage of high-resolution Landsat-7 band-8 for single-band snow cover classification. *Ann. Glaciol.*, 2002, **34**, 53–57.
31. Jain, S. K., Goswami, A. and Saraf, A. K., Accuracy assessment of MODIS, NOAA and IRS data in snow cover mapping under Himalayan conditions. *Int. J. Remote Sensing*, 2008, **29**(20), 5863–5878.
32. Macchiavello, G., Moser, G., Boni, G. and Serpico, S. B., Automatic unsupervised classification of snow-covered areas by deci-

- sion-tree classification and minimum error thresholding. *IEEE Trans. Geosci. Remote Sensing*, 2008, **44**, 2972–2982.
33. Roshani, M. J., Zouj, V., Rezaei, Y. and Nikfar, M., Snow mapping of Alamchal glacier using remote sensing data. *Int. Arch. Photogramm., Remote Sensing Inf. Sci.*, 2008, **XXXVII**, 805–808.
 34. Singh, V. P. (ed.), *Computer Models of Watershed Hydrology*, Water Resources Publications, Littleton, Colorado, 1995, p. 1130.
 35. World Meteorological Organization, Intercomparison of models of snowmelt runoff. Operational Hydrology Report 23, WMO 646, Geneva, Switzerland, 1986.
 36. Debele, B., Srinivasan, R. and Gosain, A. K., Comparison of process-based and temperature-index snowmelt modeling in SWAT. *Water Resour. Manage*, 2009; doi: 10.1007/s11269-009-9486-2
 37. Ahluwalia, R. S., Rai, S. P., Jain, S. K., Kumar, B. and Dobhal, D. P., Assessment of snowmelt run-off modelling and isotope analysis: a case study from the western Himalaya, India. *Ann. Glaciol.*, 2013, **54**(62), 299–304.
 38. Naser, S., Modelling and isotopic studies for assessment of contribution of snow/glacier melt in Parvati Basin, Himachal Pradesh. *Am. J. Geol. Ecol.*, 2013, **3**(1), 2568–5449.
 39. Dimri, T., Thakur, P. K. and Aggarwal, S. P., Energy balance approach for snowmelt run-off estimation. In Proceedings of the 99th Indian Science Congress, Bhubaneswar, 2012, p. 151.
 40. Datt, P., Srivastava, P. K., Negi, P. S. and Satyawali, P. K., Surface energy balance of seasonal snow cover for snow-melt estimation in N-W Himalaya. *J. Earth Syst. Sci.*, 2008, **117**(5), 567–573.
 41. Thakur, P. K., Duishonakunov, M., Prasad, V. H., Garg, P. K. and Garg, R. D., Hydrological study in Manali Sub-Basin of Beas River using HEC-HMS. Hydro2008, National conference on Hydraulics and Water Resources, MNIT Jaipur, 15–16 December 2008, pp. 681–693.
 42. Verdhen, A., Chahar, B. and Sharma, O., Spring time snowmelt and streamflow predictions in the Himalayan mountains. *J. Hydrol. Eng.*, 2013; 10.1061/(ASCE)HE.1943-5584.0000816
 43. Jain, S. K., Lohani, A. K. and Singh, R. D., Snowmelt run-off modeling in a basin located in Bhutan Himalaya. In India Water Week 2012 – Water, Energy and Food Security: Call for Solutions, New Delhi, 10–14 April 2012, pp. 1–13.
 44. Verdhen, A., Chahar, B. and Sharma, O., Snowmelt runoff simulation using HEC HMS in a Himalayan watershed. In World Environmental and Water Resources Congress, Cincinnati, USA, 2013, pp. 3206–3215.
 45. Shilpakar, R. B., Shakya, N. M. and Hiratsuka, A., Impact of climate change on snowmelt run-off: a case study of Tamakoshi basin in Nepal. In International Symposium on Social Management Systems, Kochi, Japan, 2009, vol. 9 (124), pp. 1–10.
 46. Arora, M., Rathore, D. S., Singh, R. D., Kumar, R. and Kumar, A., Estimation of melt contribution to total streamflow in River Bhagirathi and River Dhauli Ganga at Loharinag Pala and Tapovan Vishnugad project sites. *J. Water Resour. Protect.*, 2010, **2**, 636–643.
 47. Sati, V. P., Natural resource management and food security in the Alaknanda Basin of Garhwal Himalaya. *ENVIS Bull.*, 2008, **16**(2), 4–15.
 48. Singh, A. K. and Hasnain, S. I., Major ion chemistry and weathering control in a high altitude basin: Alaknanda River, Garhwal Himalaya, India. *Hydrol. Sci. J. Sci. Hydrol.*, 1998, **43**(6), 825–843.
 49. Jacobsen, K. and Passini, R., Analysis of ASTER GDEM elevation models. *Int. Arch. Photogramm. Remote Sensing*, 2010, **38**(1), 6.
 50. Chander, G., Markham, B. L. and Helder, D. L., Summary of current radiometric calibration for Landsat MSS, TM, ETM+ and EO-1 ALI sensors. *Remote Sensing Environ.*, 2009, **113**, 893–903.
 51. Baral, D. J. and Gupta, R. P., Integration of satellite sensor data with DEM for the study of snow cover distribution and depletion pattern. *Int. J. Remote Sensing*, 1997, **18**, 3889–3894.
 52. Singh, P., Huebl, H. and Weinmeister, H. W., Use of the recession characteristics of snowmelt hydrographs in the assessment of snow water storage in a basin. *Hydrol. Process*, 1993, **14**, 91–101.
 53. Martinec, J. and Rango, A., Parameter values for snowmelt run-off modeling. *J. Hydrol.*, 1986, **84**, 197–219.
 54. Martinec, J., Rango, A. and Major, E., *The Snowmelt-Runoff (SRM) User's Manual*, NASA Reference Publ. 1100, NASA, Washington DC, 1983.
 55. Richard, C. and Gratton, D. J., The importance of the air temperature variable for the snowmelt run-off modelling using the SRM. *Hydrol. Process.*, 2001, **15**(18), 3357–3370.
 56. Koskinen, J., Snow monitoring using microwave radars. Helsinki University of Technology Laboratory of Space Technology Espoo, Report 44, 2001.
 57. Rott, H., Prospects of microwave remote sensing for snow hydrology. In *Hydrologic Applications of Space Technology*, IAHS Publ. No. 160, 1986, pp. 215–224.
 58. Thakur, P. K., Snehamani, Prasad, V. H., Aggarwal, S. P. and Jain, S. K., Snow cover mapping using multi-sensor SAR data for parts of western Himalayas. In Proceedings of International Symposium on Snow and Avalanches, 6–10 April 2009, SASE, Manali.
- ACKNOWLEDGEMENTS. We thank Dr Y. V. N. Krishnamurthy, Director IIRS, Dehradun, Dr P. S. Roy (former Director IIRS) and Dr V. K. Dadhwal, Director, NRSC for support. Funding for this work was provided by National Action Plan on Climate Change project 'Impact of Climate and LULC change on Hydrological Regime of Ganga River Basin' as part of National Water Mission.

Received 16 April 2013; revised accepted 18 November 2013